


Article

# Nanostructured Assemblies of Gold and Silver Nanoparticles for Plasmon Enhanced Spectroscopy Using Living Biotemplates

Andressa M. Kubo<sup>1</sup>, Luiz F. Gorup<sup>1</sup>, Leonardo Toffano<sup>1</sup>, Luciana S. Amaral<sup>1</sup> ,  
Edson Rodrigues-Filho<sup>1</sup>, Haider Mohan<sup>2</sup>, Ricardo Aroca<sup>2</sup> and Emerson R. Camargo<sup>1,\*</sup>

<sup>1</sup> Department of Chemistry, UFSCar—Federal University of São Carlos, São Carlos SP 13565-905, Brazil; andressa.kubo@hotmail.com (A.M.K.); lfgorup@gmail.com (L.F.G.); leonardo.toffano@universidadebrasil.com.br (L.T.); lu\_samaral@yahoo.com.br (L.S.A.); edinho@pq.cnpq.br (E.R.F.)

<sup>2</sup> Department of Chemistry and Biochemistry, University of Windsor, Windsor, ON N9B 3P4, Canada; mohan5@uwindsor.ca (H.M.); g57@uwindsor.ca (R.A.)

\* Correspondence: camargo@ufscar.br; Tel.: +55-16-3351-8090

Received: 19 September 2017; Accepted: 1 November 2017; Published: 4 November 2017

**Abstract:** The ability to control the assembly of nanoparticles on substrates used in plasmon-enhanced spectroscopy continues to drive research in the field of nanofabrication. Here we describe the use of fungi as soft biotemplates to fabricate nanostructured microtubules with gold and gold-silver nanoparticles with potential applications as sensors and biosensors. In the first step, spores of the filamentous fungus *Cladosporium sphaerospermum* were inoculated in a suspension of gold nanoparticles, forming stable microtubules of gold nanoparticles during fungus growth. These materials were exposed to a second suspension of silver nanoparticles, resulting in complexes multilayers structures of gold and silver nanoparticles, which were evaluated as substrates for surface-enhanced Raman scattering (SERS) using small amounts of thiophenol as probe molecules directly on the microtubules. Both gold and the gold-silver substrates provide the SERS effect.

**Keywords:** surface-enhanced Raman spectroscopy; biotemplate; colloidal nanoparticles

## 1. Introduction

Gold and silver nanoparticles exhibit unique optical properties [1–3] that make them extremely useful for applications in nanoscience and nanotechnology [4,5]. In particular, gold nanoparticles have many applications in daily life, and because of their facile synthesis, easy surface functionalization, chemical stability, and biocompatibility, they have been widely used to build different nanostructured assemblies [6–8]. Silver nanoparticles, on the other hand, are popular in biomedicine because of their antimicrobial activity against several bacteria, fungi, protozoa, and certain viruses [9]. Over the last decade, new methods were developed to minimize the use and generation of hazardous substances, particularly for the synthesis of silver nanoparticles using plant extracts or juices [10]. These green routes provided a huge number of reducing and stabilizing agents [11], which opened the possibility to form new hybrid materials that combine the structural specificity of biological systems with the properties of metallic nanoparticles [12]. Several biological structures have been used as effective biotemplates for the synthesis of noble metal nanoparticles, [13,14], usually aiming to obtain nanoparticles with a fine shape control and sharp size distribution. For instance, viruses offer an excellent pattern for highly reproducible nanostructures of huge versatility [12,13,15,16], while nanoparticles of different shapes or sizes can be self-assembled into 3D molecular dynamical

structures of proteins or DNA that exhibit reconfigurable functionalities controlled by external stimuli [14].

Since gold and silver nanoparticles exhibit strong plasmon absorption bands tunable in the visible spectral region [17,18], they have become one of the most commonly material used in plasmonics, ultrasensitive detection, and surface-enhanced Raman spectroscopy (SERS) [19,20]. Although the synthesis of such small colloidal nanoparticles is relatively easy, assembling them on substrates in an ordered fashion can be challenging. Recently, hybrid structures consisting of microorganisms covered with inorganic particles have received much attention as versatile templates for the organization of nanostructured functional materials on a large scale [21,22]. The focus on the use of wet chemistry to obtain nanostructured materials is an attempt to explore the stability of colloidal nanoparticles to study hybrid materials. There are several examples regarding the use of living templates for noble metal nanoparticles, such as fungus [22,23], yeast [24], viruses [18], or supramolecular structures of biological origin [25].

Indeed, SERS sensitivity strongly depends on the optical properties of the substrate. In this context, the simultaneous attainment of good reproducibility and high-enhanced factors are key challenges in the development of improved substrates for SERS analysis [26]. Generally, SERS substrates consist of a nanostructured surface of gold or silver obtained by chemical or physical methods. Several techniques allow tuning the characteristics of surfaces for SERS, for instance through lithographic methods, precipitation from colloidal suspensions, or by the physical vapor deposition of metals on a nanostructured surface of silicon or ZnO [27]. Anisotropic metal nanoparticles, on the other hand, offer the possibility of creating “hotspots” of enhanced activity [26,28–33].

In this study, we used fungi as biotemplates to obtain self-assembled systems of gold and gold-silver nanoparticles that formed stable mesostructures with potential use as biosensors via SERS. Interestingly, microtubules fabricated exclusively with gold nanoparticles showed a uniform morphology and a smooth surface of controlled thickness, while microtubules fabricated with gold and silver nanoparticles exhibited a much rougher surface with superior potential as a substrate for SERS.

## 2. Materials and Methods

### 2.1. Synthesis

We used all of the chemicals as received without any further treatment. Gold nanoparticles (AuNPs) were synthesized using 100 mL of an aqueous solution of  $\text{HAuCl}_4$  ( $1.0 \text{ mmol}\cdot\text{L}^{-1}$ , 99.9%, Sigma-Aldrich, São Paulo, Brazil) and deionized water at  $90^\circ\text{C}$ . Then, 1 mL of a sodium citrate solution was added ( $0.30 \text{ mol}\cdot\text{L}^{-1}$ ,  $\text{Na}_3\text{C}_6\text{H}_5\text{O}_4$ ), resulting after 12 min in a stable red colloidal suspension of AuNPs. Silver nanoparticles (AgNPs) were synthesized similarly using 100 mL of an aqueous solution of  $\text{AgNO}_3$  ( $1.0 \text{ mmol}\cdot\text{L}^{-1}$ , 99.9% Sigma-Aldrich) at  $95^\circ\text{C}$  followed by the addition of 1 mL of a sodium citrate solution ( $0.30 \text{ mol}\cdot\text{L}^{-1}$ ), which resulted in a stable yellow suspension of AgNPs after approximately 12 min.

### 2.2. Formation of the Microtubules

Two different hybrid materials were prepared and characterized. The first material (hereafter referred as FG, which is an abbreviation of “fungus and gold”) was obtained by covering the filamentous fungus exclusively with gold nanoparticles, and the second material (referred to as FGS, which means “fungus, gold, and silver”) was prepared by depositing a second layer of silver nanoparticles on the first layer of gold. To prepare the first material, spores of the fungus *Cladosporium sphaerospermum* were introduced into 200 mL of a colloidal suspension of AuNPs [22]. After this inoculation, the culture media were stored for two months at room temperature and protected from light. During this period, fungi grew continuously until it achieved a size of 2 mm, suitable for use in SERS, and, simultaneously, AuNPs adhered on their walls. Half of this material, consisting of fungus-AuNP microtubules, were deposited in a silicon plate (111) and dried at room temperature

in a desiccator for several days before characterization. To obtain the second material, the aqueous solvent was partially removed from the remaining FG material, taking care to keep the mycelial mass wet, and transferred to 200 mL of a colloidal dispersion of AgNPs, which adhered on the surface of gold microtubules, forming a complex microtubule of fungus-AuNP-AgNP (FGS). The FGS sample was also isolated and dried at room temperature for several days before characterization, which caused the fungus death.

### 2.3. Characterization

Gold and silver nanoparticles were deposited on silicon by casting their respective colloidal suspensions at room temperature to be characterized by X-ray diffraction (Rigaku Dmax 2500PC diffractometer operating at 40 kV and 40 mA, Rigaku, Tokyo, Japan) with  $\text{CuK}\alpha$  radiation in  $2\theta$  range from  $20^\circ$  to  $120^\circ$ . The UV-Vis spectra of gold and silver suspensions were obtained from 190 to 800 nm using a UV-Vis spectrophotometer (JASCO V-660, Jasco, Halifax, NS, Canada). Scanning transmission electron microscopy (STEM) images of the nanoparticles were recorded at 20 kV (FEG Zeiss Supra 35-VP, Zeiss, Jena, Germany). To collect STEM images, gold and silver colloids were dripped on copper grids of 400 mesh (PELCO<sup>®</sup>), and the solvent evaporated at room temperature. Scanning electron microscopy (SEM) (FEI Company, Hillsboro, OR, USA—XL30 FEG) images were obtained using nanoparticles and microtubules deposited on a silicon plate (111). The contacts between the sample and the support were formed with conductive silver ink (Degussa). Histograms were constructed using the public domain ImageJ image processing software (version 1.50, National Institute of Health, Bethesda, MD, USA).

### 2.4. Surface-Enhanced Raman Spectroscopy (SERS)

The SERS activity of fungus-AuNP (FG) and fungus-AuNP-AgNP (FGS) microtubules were obtained by dipping them in a diluted solution of thiophenol ( $1 \times 10^{-4} \text{ mol}\cdot\text{L}^{-1}$ ) for 5 min. Using the same conditions, the spectrum of the substrate that supported the microtubules was used as a control to determine the enhancement factor of the FGS substrate for the thiophenol molecules [31,32]. The control spectrum was taken with laser powers of 1.2 mW and 2.5 mW to obtain a substantial signal of the Raman scattering of thiophenol. The presence of gold and silver was confirmed using energy dispersive spectroscopy (EDS), which indicated close values in the weight percent of both nanoparticles. Raman and SERS data were collected using a micro-Raman Renishaw InVia system with laser excitation at 633 nm and a power of 245  $\mu\text{W}$  at the sample. Spectra were collected in a backscattering geometry using a  $50\times$  microscope objective, where the probing area was ca.  $1 \mu\text{m}^2$ . The measurements were collected as 2D mappings of a computer-controlled, three-axis encoded (XYZ) motorized stage.

## 3. Results

The first experiment aimed for the formation of the FG microtubules. After the germination of the spores, monodispersed AuNPs of 25 nm began to self-organize on the surface of the hyphae, forming a reddish purple macroscopic material. This material was separated from the aqueous media without any observed mechanical damage. The sequence of images in Figure 1 shows the colloidal suspensions after 2, 30, and 45 days of incubation, illustrating the fungal growth during the experiment. A decrease in the red color of the media was evident after 60 days of incubation and the concomitant formation of the FG hybrid material.

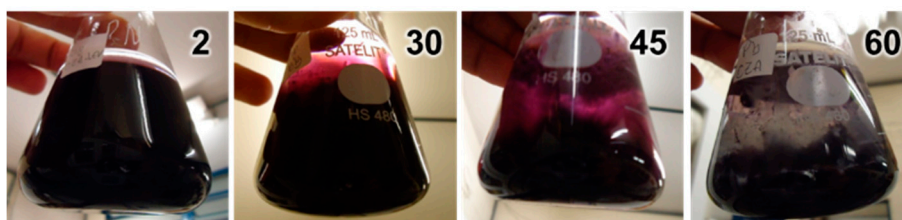


**Figure 1.** Erlenmeyer flasks containing the filamentous fungus *Cladosporium sphaerospermum* immersed in a colloidal suspension of gold nanoparticles after 2, 30, 45, and 60 days of inoculation.

Figure 2 shows SEM images of the FG sample in different magnifications. Gold nanoparticles are easily observed in the image in Figure 2a covering the fungal surface to form microtubules. Figure 2b,c shows details of the microtubule morphology, exhibiting AuNPs spread out on the fungi surface without cracks. It was also possible to observe some microtubules connected perpendicularly, resulting in structures that are almost impossible to obtain through conventional spinning processing. Figure 2d shows the uniformity of microtubules, which demonstrate the effectiveness of biotemplates to form homogeneous hybrid materials with gold nanoparticles. This image suggests a uniform density of the gold nanoparticles covering the hyphae and the formation of microtubules of equal thickness over the entire biotemplate. The long exposure of the fungus to the colloidal suspension for a couple of months probably led to an equilibrated deposition of gold nanoparticles on the filaments, even those formed in the last growth stage. After a fast growth in the beginning, the fungus growth rate decreased because of the limited amount of nutrients in a covering process that resembles a stationary state [22]. Conveniently, the interaction between the gold nanoparticles and the biotemplate was strong enough to form a self-sustained material that was easily sectioned and manipulated with simple laboratory tweezers.

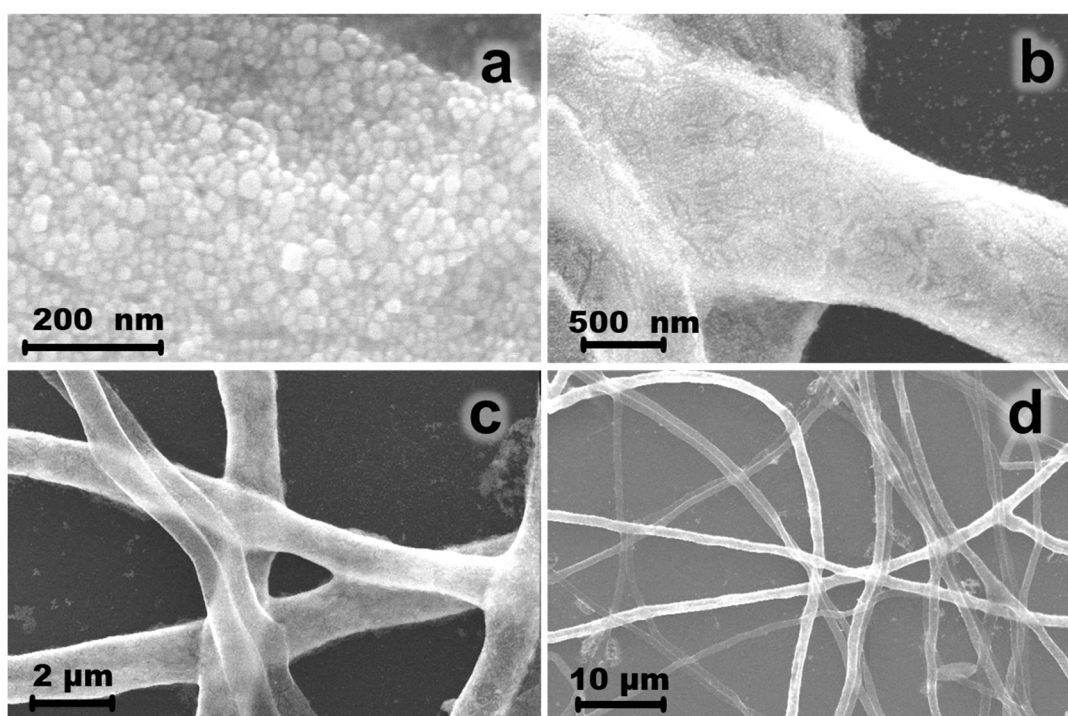


**Figure 2.** SEM images with different magnifications (a–d) of the microtubules fabricated using the fungus *Cladosporium sphaerospermum* covered with gold nanoparticles (FG) deposited on a silicon substrate.



Usually, non-covalent interactions (notably ionic or hydrogen bonds), van der Waals forces, or hydrophobic interactions drive the assembly of molecular species [34]. The first layer of AuNPs on the surface of the fungus was probably formed because of the hydrophobic effect [35], and the nanoparticles were fixed by strong covalent bonds between the metal and the proteins of the cell wall [22,23]. However, interestingly, the gold particles still formed subsequent layers due to the influence of the metabolites produced by the living fungus, since we did not observe the deposition of nanoparticles on the surface of dead fungus. During the second step of our experiment, we exposed the FG microtubules to a second suspension of AgNP aiming to obtain new microtubules with a core-shell structure of the type fungus-AuNP-AgNP (FGS). Figure 2 shows the FG sample covered by a uniform layer of AuNP, but the FGS samples in Figure 3 exhibit an irregular surface due to the AgNPs of different sizes. Point elemental analyses performed on two of the larger nanoparticles confirmed that they were essentially silver. Gorup et al. [36] reported that only about 50% of the silver ions reduce to metal colloidal suspensions of silver nanoparticles when synthesized by the citrate method. They also demonstrated that the broadening of the particle size distribution of AgNPs, even at room temperature, is due to the nucleation of new particles over time and the growth of older particles formed at the beginning. Therefore, it is possible that some of the AgNPs grew after adhering to the surface of the microtubules, which modified the size distribution of AgNPs from particles of 35 nm size on average to a broader size range, as observed in Figure 3.

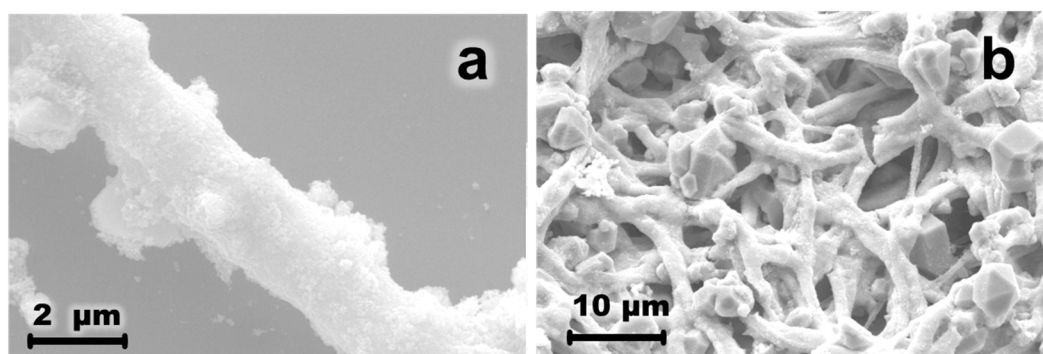


**Figure 3.** (a) SEM image of a single microtubule of *Cladosporium sphaerospermum* covered with gold and silver nanoparticles FGS. (b) SEM image of the substrate obtained with several microtubules of gold and silver nanoparticles used to collect the enhanced Raman spectrum of thiophenol.

Raman spectroscopy is an analytical technique commonly used in biomedical applications. Over the years, a wide variety of molecular targets have been investigated by SERS using active nanoparticles, mainly gold and silver [2,3,11,12,26–34]. The plasmonic origin of the phenomenon is fully understood [19,37], and nowadays the major effort focuses on the fabrication of new substrates for SERS [38]. As discussed previously (Figures 2 and 3), the FG and FGS surfaces clearly offer the necessary morphological characteristics of a typical SERS substrate. To evaluate their potential as sensors or biosensors via surface-enhanced Raman scattering, small amounts of thiophenol were used directly on FG (Figure 4a) and FGS (Figure 4b) microtubules [32,33,39–41].

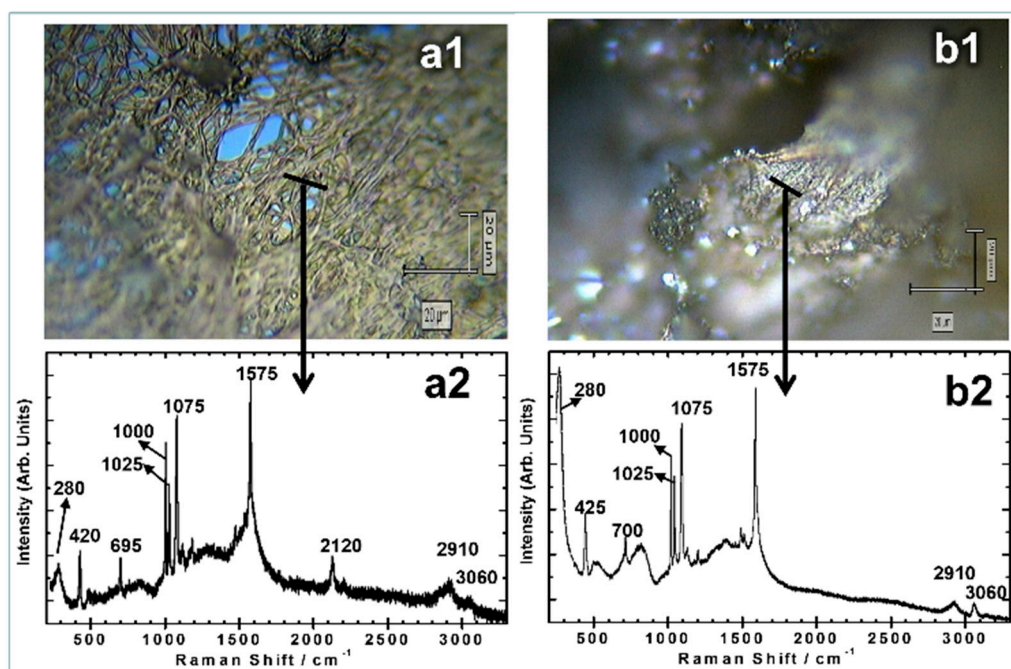


**Figure 4.** Optical images of (a1) the FG and (b1) the FGS microtubules used as substrates for surface enhanced Raman spectroscopy (SERS). The short lines on the images indicate the region analyzed. The SERS-corresponding spectra of thiophenol, obtained using a laser at 633 nm, are shown in (a2,b2). Vibrational assignments of characteristic vibrational frequencies are shown in Table 1.

**Table 1.** Vibrational assignment of thiophenol [41,42] characteristic modes observed in inelastic Raman scattering (RS) and by SERS using two different substrates.

Assignments	RS (cm <sup>-1</sup> )	SERS FG (cm <sup>-1</sup> )	SERS FGS (cm <sup>-1</sup> )
C-S stretch $\beta_{CCC}$ ( $a_1$ )	412	420	425
$\beta_{CCC'}$ vcs ( $a_1$ )	697	695	700
S-H in-plane bending	915		
$\beta_{CCC}$ ( $a_1$ )	999	1000	1000
$\beta_{CH}$ ( $a_1$ )	1024	1025	1025
$\beta_{CCC}$ ( $a_1$ )	1091	1075	1075
C = S ring stretch ( $a_1$ )	1580	1575	1575
S-H stretch	2566		

#### 4. Discussion

Compared to organic synthesis, where a virtually endless number of molecules can be synthesized by means of well-established techniques, controlling the assembly of atoms into nanocrystals is still a challenge. Chemical reactions involved in the synthesis of stable colloidal nanocrystals often appear to be simple; however, mechanisms of nucleation and growth are complex and demand new and creative solutions [36,43]. Depending on the synthesis route, nucleation mechanisms may take completely different pathways. The key to obtaining very small nanoparticles is a high density of nuclei at the beginning of the process, consuming as much of the available precursor as possible [36,44]. Each noble metal presents particular characteristics, and specific strategies of synthesis should be developed to obtain particles of different compositions and shapes. Gold, for example, is reduced almost completely, which makes it possible to control the particle size without the use of any special technique, while only a fraction of silver ions is reduced under mild conditions, leading to a broad particle size distribution [36].

The main issue in nanotechnology is the development of conceptually simple construction techniques for the fabrication of identical structures [45]. Nature builds incredibly complex and functional structures that can inspire new strategies of synthesis. Recently, the self-assembly of non-molecular components began to show potential for forming technologically useful structures. In this sense, it is particularly challenging to fuse biotechnology with chemistry to take advantage of biological components improved by evolutionary development [12,15,46]. Microorganisms, including viruses, bacteria, and fungi, grow in unique and interesting structures that can be combined with the functional properties of noble metal nanoparticles to generate new smart materials [13,16,22,23]. Usually, it is necessary to modify the surface of nanoparticles in order to increase their affinity for the mycelium [47]. However, in this study, we successfully exposed the fungi directly to colloidal suspensions of unmodified gold and silver nanoparticles, resulting in a stable hybrid material [22]. Filamentous fungi can trigger some biochemical processes in response to environmental stresses, which include the presence of Ag or Au nanoparticles in the growth media. Consequently, fungi can excrete several metabolites that are responsible for the formation of microtubules on their surface [22]. Evidently, it happens exclusively in live fungus. In fact, we observed that once isolated and dried, using for instance a freeze-dryer or simply by keeping the material inside a desiccator for several days, the fungus biotemplate lost its capacity to form new microtubules. On the other hand, both FG and FGS materials kept their mechanical stability after being dried, which allowed manipulating them with simple laboratory tweezers without any sign of degradation, even after several months. The SEM images of Figure S8 (in Supplementary Material) show with details how the microtubule is formed of several layers of gold nanoparticles.

It is now accepted that the electromagnetic enhanced mechanism is largely responsible for the SERS effect [48]. Although the contact between the analyte molecule and the substrate is not required, they should be within a certain distance from each other, which could vary from a few angstroms to tens of nanometers, in order for the SERS effect to occur. Molecules far from the substrate surface will not exhibit any enhanced signal [49], which explains the intense SERS spectra of thiophenol on the external surface of microtubules without the interference of fugus metabolites present inside the microtubules.

Thiophenol has been widely used as a molecular probe to determine the suitability of substrates for SERS and to estimate an enhancement factor due to the affinity of the thiol group (R-SH) toward noble metal surfaces [32,33]. Generally, its adsorption on gold or silver proceeds by releasing hydrogen after breaking the thiol bond. Although thiophenol molecules are intact in the gas phase, in solution they may be either intact or ionized depending on the pH. Table 1 shows the assignments of thiophenol [41,42,50–52] and their characteristic vibrations observed in the SERS spectra of Figure 4 using FG and FGS substrates. Notably, S–H stretching ( $2566\text{ cm}^{-1}$ ) and S–H bending ( $917\text{ cm}^{-1}$ ), which are present in the conventional Raman scattering (RS) spectra, disappeared in the SERS spectra of Figure 4, indicating the chemisorption of thiophenol through the rupture of the S–H bonds. Comparing the RS spectra of thiophenol reported in the literature with the SERS spectra of thiophenolate shown in Figure 4(a2 (FG), b2 (FGS)), it is evident that these SERS spectra are dominated by the symmetric  $a_1$  vibrational modes, which are normal modes with polarizability derivative components in the molecular plane. The results are in agreement with the reported SERS spectra observed by Joo et al. [41] and by Carron and Hurley [42]. For instance, the band at  $1575\text{ cm}^{-1}$ , assigned to C=C ring stretching, is less intense than the band at  $1000\text{ cm}^{-1}$  in the conventional RS spectrum [42], but appears as the most intense band in the SERS spectra obtained using FG and FGS substrates. Notably, the SERS spectra of thiophenolate using the biotemplate indicates that these new substrates based on hybrid materials are suitable to fabricate sensor devices on a large scale because of their facile production. The chemisorption takes place with the formation of the Au-S bond. Since the in-plane modes have the highest relative intensity, as can be seen in the SERS spectra of Figure 4, it can be said that the orientation of the thiophenolate is perpendicular to the surface of gold [42].

The optimization of substrates for SERS based on bimetallic nanoparticles is the subject of specialized studies [53], and several parameters must be considered. It is possible to observe FGS

microtubules as a mix of gold and silver nanoparticles that exhibit better properties and stronger SERS signals than FG samples composed of exclusively gold. The signals obtained using the FGS microtubules with AuNPs and AgNPs were one order of magnitude stronger than that obtained with the FG substrates, possibly because of the presence of a higher concentration of hot-spots formed by the irregular silver nanoparticles, which increased the average SERS intensity [20]. Evidently, the surface roughness of the FGS improved the quality of the SERS signal, and silver nanoparticles may provide higher SERS enhancement than gold nanoparticles [54], which perhaps contributed to the improved quality of the spectra obtained using FGS substrates. However, the presence of gold nanoparticles is of equal importance since it is well known that the observed enhancement of thiophenolate, among other effects, depends also on the gold content [55].

## 5. Conclusions

Studies in the field of hybrid materials can be directed toward understanding the fungi-nanoparticle interface for the construction of different structures using colloidal nanoparticles as building blocks. Our strategy was demonstrated to be an innovative method to fabricate stable self-assembled structures of gold (FS) and gold-silver (FGS) nanoparticles using the filamentous fungus *Cladosporium sphaerospermum* as a biotemplate with potential applications in biosensing via plasmon-enhanced Raman spectroscopy. The FG microtubules fabricated exclusively with AuNPs showed a uniform morphology and a smooth surface that could be reproduced on a large scale with a controlled thickness by adjusting the initial concentration of AuNPs. However, the FGS microtubules, which were obtained in two steps by the deposition of AgNPs on the surface of FG microtubules, exhibited a much rougher surface with superior potential as a substrate for surface-enhanced Raman spectroscopy.

**Supplementary Materials:** The following are available online at [www.mdpi.com/2504-5377/1/1/4/s1](http://www.mdpi.com/2504-5377/1/1/4/s1), Figure S1: Synthesis of the gold colloids synthesized at pH 3.4 and 90 °C, Figure S2: UV-Vis spectra of the gold colloids synthesized at pH 3.4 and 90 °C. The TEM image show gold nanoparticles with an average size of 25 nm, Figure S3: UV-Vis spectra of the silver colloids synthesized at pH 8.3 and 90 °C. The SEM image show silver nanoparticles with a average size of 35 nm, Figure S4: XRD pattern collected at room temperature of gold nanoparticles synthesized at 90 °C, Figure S5: XRD pattern collected at room temperature of silver nanoparticles synthesized at 90 °C, Figure S6: Erlenmeyer flasks containing mycelium of *Cladosporium sphaerospermum* and gold nanoparticles. (a) Two days after the addition of spores, (b) 30 days after the addition of spores, (c) 45 days after the addition of spores, and (d) 60 days after the addition of spore, Figure S7: SEM images of the microtubules in different magnifications of the fungus *Cladosporium sphaerospermum*, Figure S8: SEM images of microtubules obtained using fungi *Cladosporium sphaerospermum* as biotemplates for the self-assembly of gold nanoparticles showing the wall thickness with 80 nm of the microtubule, Figure S9: SEM images of the fungus *Cladosporium sphaerospermum* recovered with multilayers of gold nanoparticles (a–d) in different regions and magnifications, 2D-mapping of the elements (e) Si and (f) Au, in false color related to the SEM image “d”, Figure S10: SEM images of microtubules obtained using fungi as biotemplates for the self-assembly of gold nanoparticles showing uniformity of shape, Figure S11: SEM images and EDS with 2D-mapping of the elements Si, Ag and Au (false green, red and gray color, respectively) that compose the filamentous fungus *Aspergillus aculeatus* recovered with gold and silver nanoparticles. Hyphae were deposited on a silicon substrate, Figure S12: Optical images of (a) the FS microtubules used as SERS substrates. The short lines on the images indicate the region analyzed and (b) their respective SERS spectra of the thiophenol are shown below and were obtained using a laser at 632.8 nm, Figure S13: Optical images of (a) the FGS microtubules used as SERS substrates. The short lines on the images indicate the region analyzed, and (b) their respective SERS spectra of the thiophenol are shown below and were obtained using a laser at 632.8 nm, Figure S14: Raman signal in 514.5 nm of benzene thiol reference spectra; Raman signal of benzene thiol neat and SERS of benzene thiol with silver nanoparticles.

**Acknowledgments:** This study was supported by the Brazilian agencies FAPESP (grant 2015/13958-3 and 2013/07296-2), CNPq and CAPES. Special thanks to Aurea Maria Lage de Moraes for the fungus identification.

**Author Contributions:** L.F.G. and E.R.C. conceived and designed the experiments; A.M.K., L.F.G., L.T., and L.S.A. synthesized and characterized gold and silver nanoparticles and performed the experiments with fungi; H.M. and R.A. collected and analyzed Raman data; E.R.F. contributed reagents/materials/analysis tools; A.M.K. and E.R.C. wrote the paper.

**Conflicts of Interest:** The authors declare no conflict of interest.



## References

1. Maier, S.A. *Plasmonics: Fundamentals and Applications*; Springer: New York, NY, USA, 2007; ISBN 978-0-387-37825-1.
2. Aroca, R. *Surface-Enhanced Vibrational Spectroscopy*; John Wiley & Sons: Chichester, UK, 2006; ISBN 978-0-471-60731-1.
3. Le Ru, E.; Etchegoin, P.G. *Principles of Surface Enhanced Raman Spectroscopy*; Elsevier: Amsterdam, The Netherlands, 2009; ISBN 978-0-444-52779-0.
4. Kawata, S. Plasmonics for nanoimaging and nanospectroscopy. *Appl. Spectrosc.* **2013**, *67*, 117–125. [[CrossRef](#)] [[PubMed](#)]
5. Wang, Y.; Plummer, E.W.; Kempa, K. Foundations of plasmonics. *Adv. Phys.* **2011**, *60*, 799–898. [[CrossRef](#)]
6. Ali, M.R.K.; Snyder, B.; El-Sayed, M.A. Synthesis and optical properties of small Au nanorods using seedless growth technique. *Langmuir* **2012**, *28*, 9807–9815. [[CrossRef](#)] [[PubMed](#)]
7. Daniel, M.C.; Astruc, D. Gold nanoparticles: Assembly, supramolecular chemistry, quantum-size-related properties, and applications toward biology, catalysis, and nanotechnology. *Chem. Rev.* **2004**, *104*, 293–346. [[CrossRef](#)] [[PubMed](#)]
8. Dreaden, E.C.; Alkilany, A.M.; Huang, X.; Murphy, C.J.; El-Sayed, M.A. The golden age: Gold nanoparticles for biomedicine. *Chem. Soc. Rev.* **2012**, *41*, 2740–2779. [[CrossRef](#)] [[PubMed](#)]
9. Monteiro, D.R.; Gorup, L.F.; Silva, S.; Negri, M.; Camargo, E.R.; Oliveira, R.; Barbosa, D.B.; Henriques, M. Silver colloidal nanoparticles: Antifungal effect against adhered cells and biofilms of *Candida albicans* and *Candida glabrata*. *Biofouling* **2011**, *27*, 711–719. [[CrossRef](#)] [[PubMed](#)]
10. Sharma, V.K.; Yngard, R.A.; Lin, Y. Silver nanoparticles: Green synthesis and their antimicrobial activities. *Adv. Colloid Interface* **2009**, *145*, 83–96. [[CrossRef](#)] [[PubMed](#)]
11. Palanco, M.S.; Mogensen, K.B.; Gohlke, M.; Heiner, Z.; Kneipp, J.; Kneipp, K. Templated green synthesis of plasmonic silver nanoparticles in onion epidermal cells suitable for surface-enhanced Raman and hyper-Raman scattering. *Beilstein J. Nanotechnol.* **2016**, *7*, 834–840. [[CrossRef](#)] [[PubMed](#)]
12. Jones, M.R.; Osberg, K.D.; Macfarlane, R.J.; Langille, M.R.; Mirkin, C.A. Templated techniques for the synthesis and assembly of plasmonic nanostructures. *Chem. Rev.* **2011**, *111*, 3736–3827. [[CrossRef](#)] [[PubMed](#)]
13. Zhang, W.; Zhang, Z.P.; Zhang, X.E.; Li, F. Reaction inside a viral protein nanocage: Mineralization on a nanoparticle seed after encapsulation via self-assembly. *Nano Res.* **2017**, *10*, 3285–3294. [[CrossRef](#)]
14. Maye, M.M.; Kumara, M.T.; Nykypanchuk, D.; Sherman, W.B.; Gang, O. Switching binary states of nanoparticle superlattices and dimer clusters by DNA strands. *Nat. Nanotechnol.* **2010**, *5*, 116–120. [[CrossRef](#)] [[PubMed](#)]
15. Li, F.; Wang, Q. Fabrication of nanoarchitectures templated by virus-based nanoparticles: Strategies and applications. *Small* **2014**, *10*, 230–245. [[CrossRef](#)] [[PubMed](#)]
16. Blum, A.S.; Soto, C.M.; Wilson, C.D.; Cole, J.D.; Kim, M.; Gnade, A.; Ochoa, W.F.; Lin, T.; Johnson, J.E.; Ratna, B.R. Cowpea mosaic virus as a scaffold for 3-D patterning of gold nanoparticles. *Nano Lett.* **2004**, *4*, 867–870. [[CrossRef](#)]
17. Jain, J.K.; Huang, X.; El-Sayed, I.H.; El-Sayed, M.A. Review of some interesting surface plasmon resonance-enhanced properties of noble metal nanoparticles and their applications to biosystems. *Plasmonics* **2007**, *2*, 107–118. [[CrossRef](#)]
18. Manocchi, A.K.; Seifert, S.; Lee, B.; Yi, H. On the thermal stability of surface-assembled viral-metal nanoparticle complexes. *Langmuir* **2010**, *26*, 7516–7522. [[CrossRef](#)] [[PubMed](#)]
19. Moskovits, M. Surface-enhanced spectroscopy. *Rev. Mod. Phys.* **1985**, *57*, 783–826. [[CrossRef](#)]
20. Kleinman, S.L.; Frontiera, R.R.; Henry, A.I.; Dieringer, J.A.; Van Duyne, R.P. Creating, characterizing, and controlling chemistry with SERS hot spots. *Phys. Chem. Chem. Phys.* **1985**, *15*, 21–36. [[CrossRef](#)] [[PubMed](#)]
21. Rosi, N.L.; Thaxton, C.S.; Mirkin, C.A. Control of nanoparticle assembly using DNA-modified diatom templates. *Angew. Chem. Int. Ed.* **2004**, *43*, 5500–5503. [[CrossRef](#)] [[PubMed](#)]
22. Kubo, A.M.; Gorup, L.F.; Amaral, L.S.; Filho, E.R.; Camargo, E.R. Kinetic control of microtubule morphology obtained by assembling gold nanoparticles on living fungal biotemplates. *Bioconjug. Chem.* **2016**, *27*, 2337–2345. [[CrossRef](#)] [[PubMed](#)]

23. Bigall, N.C.; Reitzig, M.; Naumann, W.; Simon, P.; van Pée, K.-H.; Eychmüller, A. Fungal templates for noble-metal nanoparticles and their application in catalysis. *Angew. Chem. Int. Ed.* **2008**, *47*, 7876–7879. [[CrossRef](#)] [[PubMed](#)]
24. Scheibel, T.; Parthasarathy, R.; Sawicki, G.; Lin, X.M.; Jaeger, H.; Lindquist, S. Conducting nanowires built by controlled self-assembly of amyloid fibers and selective metal deposition. *Proc. Natl. Acad. Sci. USA* **2010**, *100*, 4527–4532. [[CrossRef](#)] [[PubMed](#)]
25. Zhang, T.; Wang, W.; Zhang, D.; Zhang, X.; Ma, Y.; Zhou, Y.; Qi, L. Biotemplated synthesis of gold nanoparticle–bacteria cellulose nanofiber nanocomposites and their application in biosensing. *Adv. Funct. Mater.* **2010**, *20*, 1152–1160. [[CrossRef](#)]
26. Li, W.; Zhao, X.; Glushenkov, A.M.; Kong, L. Plasmonic substrates for surface enhanced Raman scattering. *Anal. Chim. Acta* **2017**, *984*, 19–41. [[CrossRef](#)] [[PubMed](#)]
27. Barbillon, G.; Sandana, V.E.; Humbert, C.; Belier, B.; Rogers, D.J.; Teherani, F.H.; Bove, P.; McClintock, R.; Razeghi, M. Study of Au coated ZnO nanoarrays for surface enhanced Raman scattering chemical sensing. *J. Mater. Chem. C* **2017**, *5*, 3528–3535. [[CrossRef](#)]
28. Reguera, J.; Langer, J.; Aberasturi, D.J.; Liz-Marzan, L.M. Anisotropic metal nanoparticles for surface enhanced Raman scattering. *Chem. Soc. Rev.* **2017**, *46*, 3866–3885. [[CrossRef](#)] [[PubMed](#)]
29. Bryche, J.F.; Tsigara, A.; Belier, B.; Chapelle, M.L.; Canva, M.; Bartenlian, B.; Barbillon, G. Surface enhanced Raman scattering improvement of gold triangular nanoprisms by a gold reflective underlayer for chemical sensing. *Sens. Actuator B Chem.* **2016**, *228*, 31–35. [[CrossRef](#)]
30. Carrasco, S.; Benito-Pena, E.; Navarro-Villoslada, F.; Langer, J.; Sanz-Ortiz, M.N.; Reguera, J.; Liz-Marzan, L.M.; Moreno-Bondi, M.C. Multibranching gold-mesoporous silica nanoparticles coated with a molecularly imprinted polymer for label-free antibiotic surface-enhanced Raman scattering analysis. *Chem. Mater.* **2016**, *28*, 7947–7954. [[CrossRef](#)]
31. Stiles, P.L.; Dieringer, J.A.; Shah, N.C.; Van Duyne, R.P. Surface-enhanced Raman Spectroscopy. *Annu. Rev. Anal. Chem.* **2008**, *1*, 601–626. [[CrossRef](#)] [[PubMed](#)]
32. Issaad, D.; Moustou, H.; Medjahed, A.; Lalaoui, L.; Spadavecchia, J.; Bouafia, M.; Chapelle, M.L.; Djaker, N. Scattering correlation spectroscopy and Raman spectroscopy of thiophenol on gold nanoparticles: Comparative study between nanospheres and nanourchins. *J. Phys. Chem. C* **2017**, *121*, 18254–18262. [[CrossRef](#)]
33. Biggs, K.; Camden, J.P.; Anker, J.N.; Van Duyne, R.P. Surface-enhanced Raman spectroscopy of benzenethiol adsorbed from the gas phase onto silver film over nanosphere surfaces: Determination of the sticking probability and detection limit time. *J. Phys. Chem. A* **2009**, *113*, 4581–4586. [[CrossRef](#)] [[PubMed](#)]
34. Lee, P.C.; Meisel, D. Adsorption and surface-enhanced Raman of dyes on silver and gold sols. *J. Phys. Chem.* **1982**, *86*, 3391–3395. [[CrossRef](#)]
35. Zhang, S. Fabrication of novel biomaterials through molecular self-assembly. *Nat. Biotech.* **2003**, *21*, 1171–1178. [[CrossRef](#)] [[PubMed](#)]
36. Sugunan, A.; Melin, P.; Schnürer, J.; Hilborn, J.G.; Dutta, J. Nutrition-driven assembly of colloidal nanoparticles: Growing fungi assemble gold nanoparticles as microwires. *Adv. Mater.* **2007**, *19*, 77–81. [[CrossRef](#)]
37. Gorup, L.F.; Longo, E.; Leite, E.R.; Camargo, E.R. Moderating effect of ammonia on particle growth and stability of quasi-monodisperse silver nanoparticles synthesized by the Turkevich method. *J. Colloid Interface Sci.* **2011**, *360*, 355–358. [[CrossRef](#)] [[PubMed](#)]
38. Moskovits, M. Persistent misconceptions regarding SERS. *Phys. Chem. Chem. Phys.* **2013**, *15*, 5301–5311. [[CrossRef](#)] [[PubMed](#)]
39. Fan, M.; Andrade, G.F.S.; Brolo, A.G. A review on the fabrication of substrates for surface enhanced Raman spectroscopy and their applications in analytical chemistry. *Anal. Chim. Acta* **2011**, *693*, 7–25. [[CrossRef](#)] [[PubMed](#)]
40. Gunnarsson, L.; Bjerneld, E.J.; Xu, H.; Petronis, S.; Kasemo, B.; Käll, M. Interparticle coupling effects in nanofabricated substrates for surface-enhanced Raman scattering. *Appl. Phys. Lett.* **2001**, *78*, 802–804. [[CrossRef](#)]
41. Joo, T.H.; Kim, M.S.; Kim, K. Surface-enhanced Raman scattering of 2-butanethiol in silver sol. *J. Raman Spectrosc.* **1987**, *160*, 81–89. [[CrossRef](#)]

42. Carron, K.T.; Hurley, L.G. Axial and azimuthal angle determination with surface-enhanced Raman spectroscopy: Thiophenol on copper, silver, and gold metal surfaces. *J. Phys. Chem.* **1991**, *95*, 9979–9984. [[CrossRef](#)]
43. Xia, Y.; Xiong, Y.; Lim, B.; Skrabalak, S.E. Shape-controlled synthesis of metal nanocrystals: Simple chemistry meets complex physics? *Angew. Chem. Int. Ed.* **2009**, *48*, 60–103. [[CrossRef](#)] [[PubMed](#)]
44. LaMer, V.K.; Dinegar, R.H. Theory, production and mechanism of formation of monodispersed hydrosols. *J. Am. Chem. Soc.* **1950**, *72*, 4847–4854. [[CrossRef](#)]
45. Juárez, J.; Cambón, A.; Topete, A.; Taboada, P.; Mosquera, V. One-dimensional magnetic nanowires obtained by protein fibril biotemplating. *Chem. Eur. J.* **2011**, *17*, 7366–7373. [[CrossRef](#)] [[PubMed](#)]
46. Niemeyer, C.M. Nanoparticles, proteins, and nucleic acids: Biotechnology meets materials science. *Angew. Chem. Int. Ed.* **2001**, *40*, 4128–4158. [[CrossRef](#)]
47. Fakhruddin, R.F.; Zamaleeva, A.I.; Morozov, M.V.; Tazetdinova, D.I.; Alimova, F.K.; Hilmutdinov, A.K.; Zhdano, R.I.; Kahraman, M.; Culha, M. Living fungi cells encapsulated in polyelectrolyte shells doped with metal nanoparticles. *Langmuir* **2009**, *25*, 4628–4634. [[CrossRef](#)] [[PubMed](#)]
48. Heynes, C.L.; Yonzon, C.R.; Zhang, X.; Van Duyne, R.P. Surface-enhanced Raman sensors: Early history and the development of sensors for quantitative biowarfare agent and glucose detector. *J. Raman Spectrosc.* **2005**, *36*, 471–484. [[CrossRef](#)]
49. Dieringer, J.A.; McFarland, A.D.; Shah, N.C.; Stuart, D.A.; Whitney, A.V.; Yonzon, M.A.; Young, M.A.; Zhang, X.; Van Duyne, R.P. Surface enhanced Raman spectroscopy: New materials, concepts, characterization tools, and applications. *Faraday Discuss.* **2006**, *132*, 9–26. [[CrossRef](#)] [[PubMed](#)]
50. Jana, N.R.; Gearheart, L.; Murphy, C.J. Seeding growth for size control of 5–40 nm diameter gold nanoparticles. *Langmuir* **2001**, *17*, 6782–6786. [[CrossRef](#)]
51. Han, S.W.; Lee, S.J.; Kim, K. Self-assembled monolayers of aromatic thiol and selenol on silver: comparative study of adsorptivity and stability. *Langmuir* **2001**, *17*, 6981–6987. [[CrossRef](#)]
52. Taylor, C.E.; Pemberton, J.E.; Goodman, G.G.; Schoenfish, M.H. Surface enhancement factors for Ag and Au surfaces relative to Pt surfaces for monolayers of thiophenol. *Appl. Spectrosc.* **1999**, *53*, 1212–1221. [[CrossRef](#)]
53. Fan, M.; Lai, F.J.; Chou, H.L.; Lu, W.T.; Hwang, B.J.; Brolo, A.G. Surface-enhanced Raman scattering (SERS) from Au:Ag bimetallic nanoparticles: The effect of the molecular probe. *Chem. Sci.* **2013**, *4*, 509–515. [[CrossRef](#)]
54. Herrera, G.; Padilla, A.; Hernandez-Rivera, S. Surface enhanced Raman scattering (SERS) studies of gold and silver nanoparticles prepared by laser ablation. *Nanomaterials* **2013**, *3*, 158–172. [[CrossRef](#)] [[PubMed](#)]
55. Holze, R. The adsorption of thiophenol on gold—A spectroelectrochemical study. *Phys. Chem. Chem. Phys.* **2015**, *17*, 21364–21372. [[CrossRef](#)] [[PubMed](#)]

